Acoustics'08 Paris
June 29-July 4, 2008
www.acoustics08-paris.org

Single parameter description of seafloors for shallow oceans

Adrian Jones, Graham Day and Paul Clarke

Defence Science and Technology Organisation, P.O Box 1500, 5111 Edinburgh, Australia
adrian.jones@dsto.defence.gov.au

For a shallow ocean, sound transmission beyond short range is dominated by seafloor interactions at small grazing angles β, for which the loss in dB on each bottom reflection may be approximated by a function *F*β where *F* dB/radian is a constant. Acoustic inversion techniques exist which have been shown to obtain the value *F* for a particular frequency. The suitability of this single parameter as a seafloor descriptor has been re-visited for a range of seafloor types. It is shown that if the phase angle for a seafloor reflection is linked to the parameter *F* via a simple approximation, the phase-coherent properties of the shallow water interference field may be estimated to an accuracy which is expected to satisfactory for some purposes. This paper reviews the relevant theory and presents comparisons between *TL* predicted using full geoacoustic parameters versus *TL* based on the single parameter, for both uniform half-space and layered seafloor types.

1 Introduction

For small grazing angles β, typical of shallow water transmission, it is well established that the loss in dB on each bottom reflection may be approximated as proportional to the grazing angle, e.g. as stated by Urick [1]. The bottom loss then becomes *F*β dB, where the "bottom loss slope", *F* dB/radian, is a single parameter which describes the seafloor. This is explained, for example, by Weston [2] in terms of bottom impedance, and was used in the derivation of several depth-averaged transmission loss expressions for the "mode stripping zone", e.g. [2, 3]. This simplified description of bottom loss function has been incorporated in studies of shallow water transmission, reverberation and signal excess by Harrison [4]. It has also been used in studies of the spatial statistics of the interference field in a shallow ocean [5, 6].

The determination, by measurement, of the bottom loss slope parameter *F* was first proposed and used by Smith [7], and more recently by Harrison [4], in terms of an impulse response. Jones et al [8] also have developed and demonstrated a technique to obtain *F* from measurement using a broadband method.

As the authors had gained recent experience in obtaining the bottom loss slope *F* dB/radian through inversion of at-sea data [8], it was considered appropriate to investigate its use as a preferred parameter to describe seafloors in shallow oceans, and for phase coherent calculations in particular. An obvious limitation in the use of parameter *F* includes the need for the seafloor to not be acoustically rough, for which a non-linear variation of bottom loss with grazing angle may apply. This work is then relevant to seafloors which are acoustically smooth.

2 Seafloor Description

For present purposes it will be assumed to be understood that the bottom loss in dB at shallow angles is very nearly a linear function of grazing angle. For phase incoherent calculations of Transmission Loss (*TL*), the single parameter *F* is all that is required to describe the seafloor. For phase-coherent calculations, a phase angle function is required. At the Defence Science and Technology Organisation (DSTO), a simple, but satisfactory, description has been obtained, as shown below.

2.1 Reflection Phase Angle

For plane wave reflection from a lossless fluid boundary, the reflection phase change may be shown to be (e.g. see Brekhovskikh and Lysanov [9]

$$\varphi = -2\arctan\left[\frac{\sqrt{\cos^2\beta - n_r^{\,2}}}{m\sin\beta}\right] \text{ radians.} \qquad (1)$$

where φ is reflection phase angle, radians

β angle of incidence on seafloor, radians

$m = \rho_b/\rho_w$

$n_r = c_w/c_b$, index of refraction

c_b speed of sound in sub-bottom, m/s

c_w speed of sound in seawater, m/s

ρ_b density of ocean bottom, kg/m^3

ρ_w density of sea water, kg/m^3

If the grazing angle β is small, $\sin\beta \approx \beta$ and is small, and the above expression is of an arctangent of a number » 1. Now $\arctan x = (\pi/2) - (1/x) + (1/3x^3) - \ldots \approx (\pi/2) - (1/x)$ for *x* large and +ve, so we may approximate the above expression as

$$\varphi \approx -\pi + \frac{2\,m\sin\beta}{\sqrt{\cos^2\beta - n_r^{\,2}}} \approx -\pi + \frac{2\,m\,\beta}{\sqrt{1 - n_r^{\,2}}} \text{ radians.} \qquad (2)$$

Eqs.(1) and (2) show the phase angle on reflection at zero grazing angle as -π radians. For progressively increased angles of incidence, the reflection phase angle decreases (in amplitude) to zero at $\beta_c = \arccos(c_w/c_b) = \arccos(n)$, where β_c is the critical angle. From (2), we see that the phase of the reflection varies from -π, at zero grazing angle, in a function which is close to linear in grazing angle β, at least for small β. Although no proof will be presented here, it will be expected that, for realistic seafloors which incorporate lossy transmission, a similar variation of reflection phase occurs at shallow angles.

For application to lossy seafloors, the authors have found it effective to assume such a linear variation of reflection phase angle, and, further, to assume that the reflection phase reaches zero at the critical angle β_c where this is estimated as that grazing angle for which bottom loss is 6 dB. In this way, a value of bottom loss function *F* leads to a complete description of a seafloor for input to a phase coherent transmission model. For lossy seafloors, Joseph [10] had shown earlier that, for shallow grazing angles, both the bottom loss and reflection phase are approximate linear functions of grazing angle. Further, Joseph proposed that each be determined separately in a measurement requiring a spatial aperture. Such an approach will be expected to provide a more accurate description than that described in this paper, however, as shown in section 3, the authors' single parameter description is nonetheless satisfactory for many practical purposes and permits the use of a simpler inversion measurement to obtain the parameter.

3 Transmission Loss Simulations

The approach described above provides a description of the seafloor based on merely one parameter: *F*. The adequacy of this description is now illustrated by several examples of a comparison of *TL* predicted using a full knowledge of the seafloor with *TL* predicted using the simple seafloor model.

3.1 Uniform half-space

3.1.1 Soft sedimentary rock seafloor

Fig. 1 shows the bottom loss and reflection phase values, as a function of grazing angle, for a seafloor of soft sedimentary rock (seafloor type F of Desharnais and Chapman [11]), for which geoacoustic properties were assumed as shown in Table 1, and an acoustic frequency of 1000 Hz was assumed. The reflection characteristics shown in Fig. 1 were obtained using values for seawater at the ocean bottom of c_w = 1496.15 m/s, ρ_w = 1000 kg/m3, attenuation 7.6×10-5 dB/λ.

density (kg/m^3)	c_p (m/s)	c_s (m/s)	α_p (dB/λ)	α_s (dB/λ)
2100	2300	850	0.23	0.17

Table 1 Seafloor Properties: Soft Sedimentary Rock [11]

where c_p compressional wave speed (bottom), m/s

c_w shear wave speed (bottom), m/s

α_p compressional wave attenuation (bottom), dB/λ

α_s shear wave attenuation (bottom), dB/λ

The blue curves in Fig. 1 show the bottom loss and reflection phase as determined by a bottom reflection model using the seafloor parameters in Table 1. The red dashed line in the upper part of Fig. 1 is drawn to match the slope of the blue curve at small grazing angles – a slope *F* = 21.9 dB/radian provides a good match. The red dashed curve in the lower part of Fig. 1 was obtained using the technique outlined in the previous section of this paper. Phase coherent *TL* was determined using the KRAKENC (modal) model, using (i) geacoustic parameters as direct inputs, (ii) the simplified bottom loss and phase angle curves as direct inputs, for source and receiver depths 18.3 m and frequency 1000 Hz. The ocean was assumed to be range-independent, to have a seafloor as described in Fig. 1, a depth of 225 m, and to have a sound speed profile (SSP) typical of summer conditions in Australia's northern shallow waters. The assumed SSP is shown in Fig. 2 and the *TL* calculations to 20 km are shown in Fig. 3.

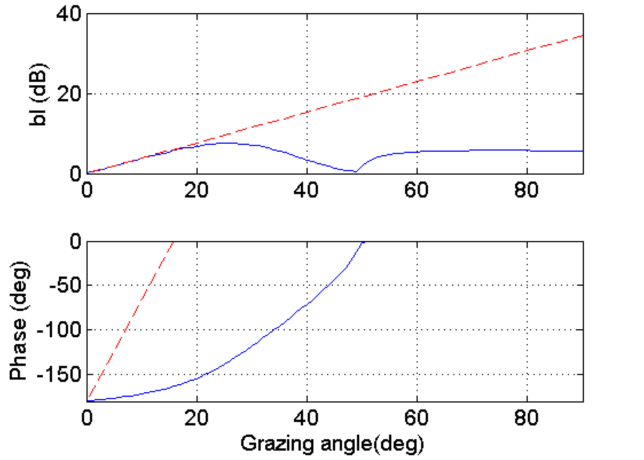

Fig.1 Seafloor bottom loss & phase angle – soft sedimentary rock 1000 Hz, **-** full description, **- -** description based on *F*

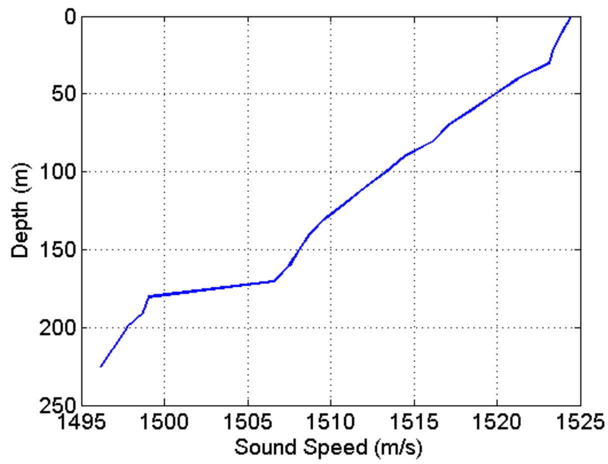

Fig.2 Summer SSP

The data in Fig. 3 show that the *TL* is virtually the same whether the full description of the seafloor is used, or whether the simplified description, based on the parameter *F*, is used. In the data within Fig. 3, there is little difference in the details of the *TL* versus range data, and no effective difference in range-averaged data, as judged by eye. The detailed *TL* at very short range does show that the simplified result does not replicate the values obtained with the geoacoustic seafloor description, most likely due the to differences between the bottom loss curves at grazing angles > 20° (Fig. 1). The seafloor parameters in Table 1 include a high shear speed, which may be shown to cause the bottom loss to decrease as grazing angle exceeds about 30°. At steeper grazing angles, the assumption adopted in this study, of a linear increase in bottom loss with grazing angle, gives rise to bottom loss values quite different to those obtained using the geoacoustic seafloor description, however it is clear that the practical significance of the difference is nil, except at very short range.

If one bears in mind the extent to which the true geoacoustic parameters may ever be known for a real seafloor, it may be argued that the simple seafloor description in Fig. 1 is quite adequate.

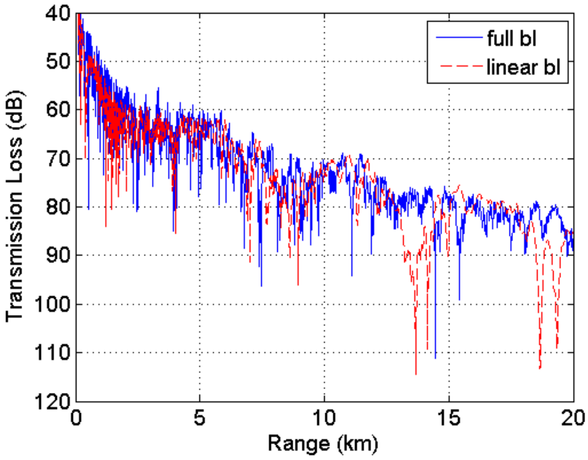

Fig.3 *TL* - soft sedimentary rock seafloor, summer SSP, source & receiver depths 18.3 m, 1000 Hz, - full description, - - description based on *F*

This comparison was repeated for different frequencies with much the same result. Fig. 4 shows results for a low frequency: 100 Hz. The results in Fig. 4 were calculated using the KRAKENC model, as for the previous case.

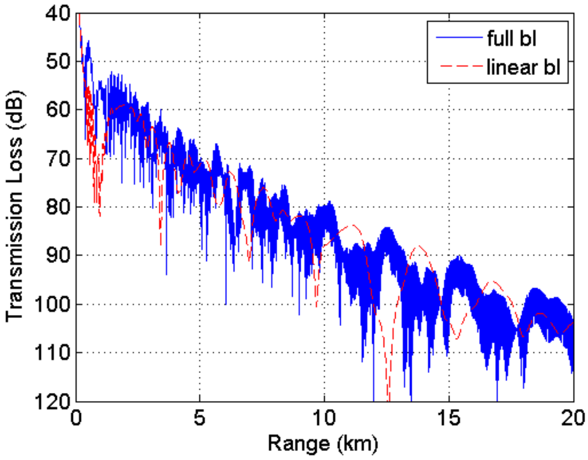

Fig.4 *TL* - soft sedimentary rock seafloor, summer SSP, source & receiver depths 18.3 m, 100 Hz, - full description, - - description based on *F*

Fig. 4 shows that mean values of *TL* are still well predicted, however, the simple assumption no longer leads to an adequate description of the detail of the interference field.

3.1.2 Silt seafloor

The modelling exercise was repeated for a seafloor of silt (seafloor type A of Desharnais and Chapman [11]), for which geoacoustic properties were assumed as shown in Table 2, at an acoustic frequency of 1000 Hz. The reflection characteristics shown in Fig. 5 (solid blue curves) were obtained using the assumed values for seawater described in the previous section.

Density (kg/m^3)	c_p (m/s)	c_s (m/s)	α_p (dB/λ)	α_s (dB/λ)
1600	1550	125	0.78	0.25

Table 2 Seafloor Properties: Silt [11]

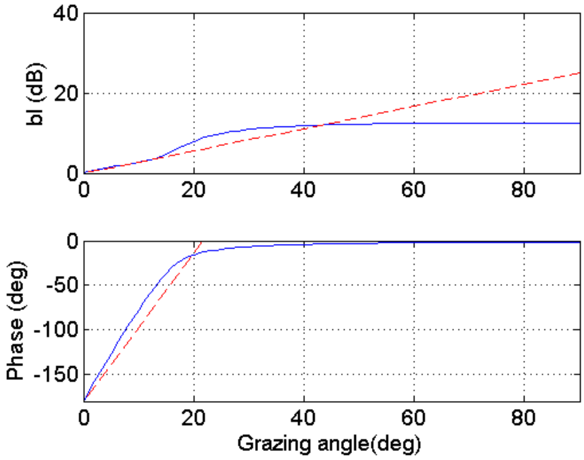

Fig.5 Seafloor bottom loss & phase angle – silt 1000 Hz, - full description, - description based on *F*

The blue curves in Fig. 5 show the bottom loss and reflection phase as determined using the seafloor parameters in Table 2. The red dashed line in the upper part of Fig. 5 is drawn to match the slope of the blue curve at small grazing angles – a slope F = 15.9 dB/radian. The red dashed curve in the lower part of Fig. 1 was obtained using the technique outlined in this paper. For each seafloor description, *TL* was determined using the KRAKENC model as described in Section 3.1.1, for source and receiver depths 18.3 m, at 1000 Hz. The ocean was assumed to be range-independent, to have a seafloor as described in Fig. 5, with depth and SSP as for the previous example (ref. Fig. 2). Phase coherent *TL* calculations to 20 km are shown in Fig. 6.

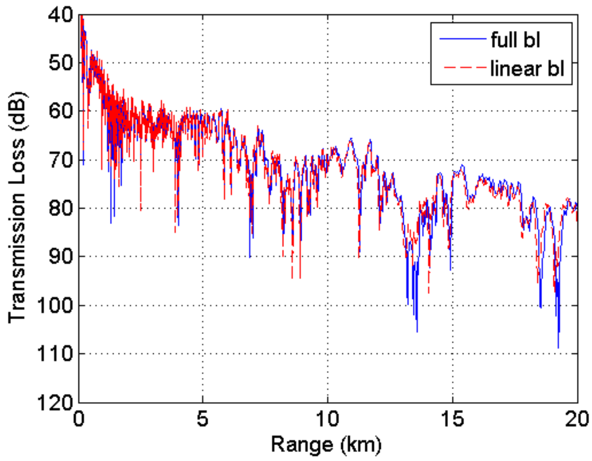

Fig.6 *TL* - silt seafloor, summer SSP, source & receiver depths 18.3 m, 1000 Hz, - full description, - - description based on *F*

This comparison was repeated for different frequencies, with one result shown below: Fig. 7 shows *TL* calculations at 100 Hz. The results in Fig. 7 were obtained using the KRAKENC model, as described in Section 3.1.1, for source and receiver depths 18.3 m.

The data in Fig. 7 shows that the *TL* is virtually identical whether the full description of the seafloor is used, or whether the simplified description, based on the parameter *F*, is used. This might be expected, based on the small degree of difference shown by the bottom loss and phase curves in Fig. 5, but is remarkable, nonetheless.

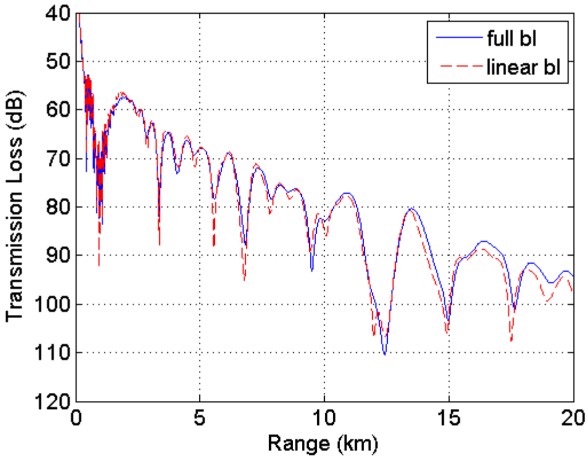

Fig.7 *TL* - silt seafloor, summer SSP, source & receiver depths 18.3 m, 100 Hz, - full description, - description based on *F*

3.2 Layered seafloor – sand/limestone

The adequacy of the single parameter description was investigated for an example of a layered seafloor. The example chosen, which is believed to be representative of some seafloors in the Australian region (e.g. ref. [8]) is a 0.3 m layer of sand over a limestone halfspace. For present purposes, the geoacoustic properties used to describe this seafloor are as shown in Table 3. The properties for fine sand correspond to Desharnais and Chapman's seafloor type B, whereas the properties for limestone correspond with those of Jensen et al [12], page 38.

	Density (kg/m^3)	c_p (m/s)	c_s (m/s)	α_p (dB/λ)	α_s (dB/λ)
fine sand	1700	1700	200	0.60	0.25
limestone	2400	3000	1500	0.10	0.20

Table 3 Seafloor Properties: Fine Sand [11], Limestone [12]

For this seafloor, simulations were carried out at two frequencies: 100 Hz and 400 Hz. Curves of bottom loss and reflection phase produced by a bottom reflection model are shown as the solid blue lines in Figs. 8 and 9 using the seafloor parameters in Table 3.

The red dashed line in the upper part of Fig. 8 is drawn to match the slope of the blue curve at small grazing angles – a slope $F = 60$ dB/radian provides a good match. From Fig. 9, for 400 Hz a slope of 23 dB/radian was selected. The red dashed curves in the lower parts of Figs. 8 and 9 were obtained using the technique outlined earlier. For each seafloor description, *TL* at each frequency was determined using the KRAKENC model, as described in Section 3.1.1, for source and receiver depths 18.3 m. The ocean environments were assumed to be range-independent, with ocean depth and SSP as for the previous examples. The phase coherent *TL* values determined are shown in Figs. 10 and 11.

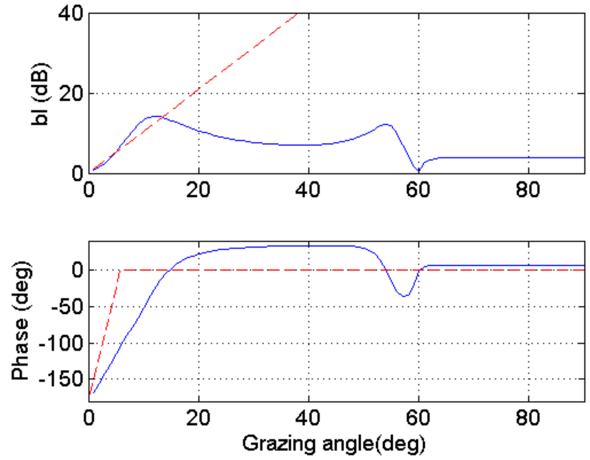

Fig.8 Seafloor bottom loss & phase angle – layered seafloor 100 Hz, - full description, - - description based on *F*

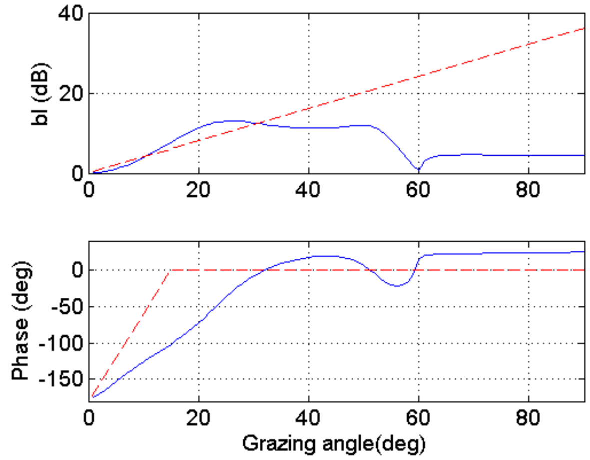

Fig.9 Seafloor bottom loss & phase angle – layered seafloor 400 Hz, - full description, - - description based on *F*

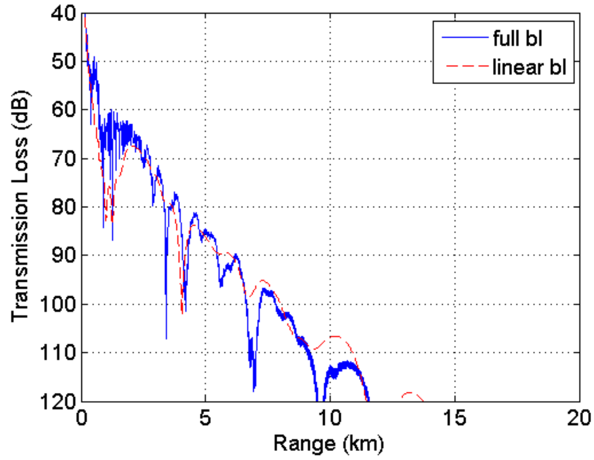

Fig.10 *TL* - layered seafloor, summer SSP, source & receiver depths 18.3 m, 100 Hz, - full description, - - description based on *F*

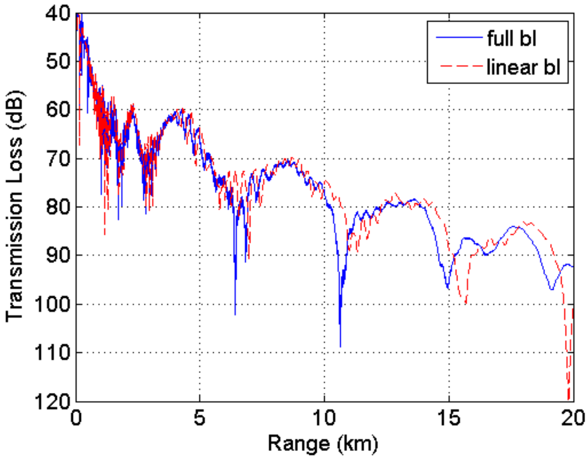

Fig.11 *TL* - layered seafloor, summer SSP, source & receiver depths 18.3 m, 400 Hz, - full description, - - description based on *F*

4 Discussion

The three seafloor types selected for study are representative of the large number for which simulations have been carried out by the authors. Clearly, the low shear speed silt seafloor well demonstrates the authors' thesis. However, the soft sedimentary rock seafloor represents a "poor" fit to the authors' assumption of both bottom loss and phase, yet the impact of this on the transmission loss calculation is minimal. In this case, there is a gradual rise in bottom loss from zero degrees grazing (Fig. 1), due to energy carried into the seafloor by shear waves, but a dip in bottom loss at the critical angle $\theta_c = \arccos(c_w / c_p)$ [13].

The fine sand-over-limestone seafloor may be expected to resemble a high shear speed material at low frequency (Fig. 8), and to resemble more closely an absorbing fluid seabed at higher frequency (Fig. 9). The simple seafloor description is adequate at both frequency ranges for this seafloor, and, in fact, provides an adequate description for all cases presented here.

It might be expected that sound transmission from a directional source may be underestimated by the proposed method, if that sound is directed at certain steep grazing angles toward elastic seabeds. Short ranges, likewise will be subject to less accurate transmission predictions as steeper angled arrivals are more significant. Further, if seafloor roughness causes the variation of bottom loss with small grazing angle to cease adhering to a linear function, the method proposed here may be in error. However, if a pragmatic view is taken with regard to the knowledge one is likely to have about some real seafloors, the single parameter approach shown here has merit. Improvements to the method are feasible if some extra information is known, in particular, in regard to the critical angle for the seafloor, but this is not considered here.

5 Conclusions

This paper re-visits the application of the slope of the bottom loss versus grazing angle function, *F* dB/radian, to the description of the significant acoustic effects of a seafloor in a shallow ocean. By incorporating an approximation, it has been shown how the corresponding variation of reflection phase may be described, and thus, the detail of the interference field may be estimated. It is acknowledged that this phase assumption is crude, yet the ability to describe the sound transmission is, nonetheless, expected to be adequate for some purposes, especially considering the likelihood of full geoacoustic descriptions for real seafloors being obtained in practical circumstances.

References

[1] R.J. Urick, "Intensity Summation of Modes and Images in Shallow-Water Sound Transmission" *J. Acoust. Soc. Am.* 46, No. 3 (Part 2), 780-788 (1969)

[2] D.E. Weston, "Intensity-range relations in oceanographic acoustics", *J. Sound Vibration* 18(2), 271-287 (1971)

[3] M. Schulkin and J.A. Mercer, "Colossus Revisited: A Review and Extension of the Marsh-Schulkin Shallow Water Transmission Loss Model (1962)", *APL-UW* 8508 (1985)

[4] C.H. Harrison, "Closed-form expressions for ocean reverberation and signal excess with mode stripping and Lambert's law", *J. Acoust. Soc. Am.* 114(5), 2744-2756 (2003)

[5] P.W. Smith, Jr., "Spatial coherence in multipath or multimodal channels", *J. Acoust. Soc. Am.* 60, No. 2, 305-310 (1976)

[6] A.D. Jones, A.J. Duncan and A.L. Maggi "Robust Prediction of Spatial Statistics of Acoustic Field for Shallow Oceans", *2nd International Conference and Exhibition on Underwater Acoustic Measurements: Technologies and Results*, Crete, 195–200 (2007)

[7] P.W. Smith, Jr., "The Averaged Impulse Response of a Shallow-Water Channel", *J. Acoust. Soc. Am.* 50, No. 1 (Part 2), 332-336 (1971)

[8] A.D.Jones, J.Hoffman and P.A.Clarke "Seafloor Reflectivity – A Test of an Inversion Technique", *Proceedings of Australian Acoustical Society Annual Conference 2000*, Western Australia, 301–305 (2000)

[9] L.M. Brekhovskikh and Yu. P. Lysanov, "Fundamentals of Ocean Acoustics", 2nd edition, Springer-Verlag (1991)

[10] P.Joseph, "Complex reflection phase gradient as an inversion parameter for the prediction of shallow water propagation and the characterisation of sea-bottoms" , *J. Acoust. Soc. Am.* 113, No. 2, 758-768 (2003)

[11] F. Desharnais and D.M.F. Chapman "Vertical Coherence of the Shallow Water Ambient Noise Field", Technical Memorandum DREA TM 1999-011, DREA, Canada (1999)

[12] F.B.Jensen, W.A.Kuperman, M.B.Porter and H.Schmidt, "Computational Ocean Acoustics", Springer-Verlag (2000)

[13] L.M. Brekhovskikh, "Waves in Layered Media", 2nd edition, Academic Press (1980)